HHS Public Access

Author manuscript

Medchemcomm. Author manuscript; available in PMC 2015 July 07.

Published in final edited form as:

Medchemcomm. 2013 May 30; 4: 1156–1165. doi:10.1039/C3MD00132F.

4-Alkyloxyimino-cytosine nucleotides: tethering approaches to molecular probes for the $P2Y_6$ receptor†

P. Suresh Jayasekara[a], **Matthew O. Barrett**[b], **Christopher B. Ball**[b], **Kyle A. Brown**[b], **Eszter Kozma**[a], **Stefano Costanzi**[c], **Lucia Squarcialupi**[a], **Ramachandran Balasubramanian**[a], **Hiroshi Maruoka**[a], and **Kenneth A. Jacobson**[a]

Kenneth A. Jacobson: kajacobs@helix.nih.gov

[a]Molecular Recognition Section, Laboratory of Bioorganic Chemistry, National Institute of Diabetes and Digestive and Kidney Diseases, National Institutes of Health, Bethesda, MD 20892-0810, USA. Fax: +1 301-480-8422; Tel: +1 301-496-9024

[b]Department of Pharmacology, University of North Carolina, School of Medicine, Chapel Hill, North Carolina 27599-7365, USA

[c]Department of Chemistry, American University, Washington, DC 20016, USA

Abstract

4-Alkyloxyimino derivatives of pyrimidine nucleotides display high potency as agonists of certain G protein-coupled P2Y receptors (P2YRs). In an effort to functionalize a $P2Y_6R$ agonist for fluorescent labeling, we probed two positions (N^4 and γ-phosphate of cytidine derivatives) with various functional groups, including alkynes for click chemistry. Functionalization of extended imino substituents at the 4 position of the pyrimidine nucleobase of CDP preserved $P2Y_6R$ potency generally better than γ-phosphoester formation in CTP derivatives. Fluorescent Alexa Fluor 488 conjugate **16** activated the human $P2Y_6R$ expressed in 1321N1 human astrocytoma cells with an EC_{50} of 9 nM, and exhibited high selectivity for this receptor over other uridine nucleotide-activated P2Y receptors. Flow cytometry detected specific labeling with **16** to $P2Y_6R$-expressing but not to wild-type 1321N1 cells. Additionally, confocal microscopy indicated both internalized **16** ($t_{1/2}$ of 18 min) and surface-bound fluorescence. Known $P2Y_6R$ ligands inhibited labeling. Theoretical docking of **16** to a homology model of the $P2Y_6R$ predicted electrostatic interactions between the fluorophore and extracellular portion of TM3. Thus, we have identified the N^4-benzyloxy group as a structurally permissive site for synthesis of functionalized congeners leading to high affinity molecular probes for studying the $P2Y_6R$.

Introduction

The $P2Y_6$ receptor ($P2Y_6R$) belongs to a family of eight G protein-coupled receptors (GPCRs) activated by extracellular nucleotides.[1] The $P2Y_6R$, which is both cytoprotective and proinflammatory, promotes inositol lipid signaling through G_q mediated activation of phospholipase C-β (PLC-β) isozymes and is found in intestinal epithelial, endocrine, skeletal

†Electronic supplementary information (ESI) available. See DOI: 10.1039/c3md00132f

Correspondence to: Kenneth A. Jacobson, kajacobs@helix.nih.gov.

muscle, bone, neuronal, vascular, immune and other cells.[1–10] Pharmacological modulation of the $P2Y_6R$ has been proposed to be useful in treatment of osteoporosis, neurodegeneration, gout, ocular hypertension, glaucoma, inflammation, intestinal disorders, diabetes, and other diseases.[2–10]

Uridine 5′-diphosphate (UDP **1**) is the endogenous $P2Y_6R$ agonist (EC_{50} = 0.30 μM), and various structure activity relationship (SAR) studies have identified sites for modification of UDP that improve its potency and/or selectivity (Chart 1).[11–17] Potent $P2Y_6R$ agonists (EC_{50} values, nM) include 3-phenacyl-UDP **2** (70),[11] derivatives of the 5 position **3** (15) and **4** (300),[12,13] a bicyclic analogue **5** (MRS2795, 42) of UDP that maintains a South (S) conformation of the ribose-like ring,[14] N^4-benzyloxy-CDP **6** (MRS2964, 26) and various dinucleoside triphosphates, [14–16] including Up_3U **7** (270), N^4-methoxy-Cp_3U **8** (MRS2957, 12), and INS48823 **9** (130). Here, we considered structural extensions of UDP that would both preserve $P2Y_6R$ agonist potency and permit the coupling of reporter groups or other large chemical carrier moieties. A functionalized congener approach to ligand derivatization has been explored for a variety of GPCRs, leading to fluorescent probes,[18] affinity labels, cross-linking ligands, and specialized radioactive probes.[39] SAR analyses suggested that the steric constraints of the pharmacophoric binding site of the receptor likely could be circumvented by chain elongation through two specific sites in $P2Y_6R$ agonists. Thus, we introduced a 4-alkyloxyimino group in the nucleobase, and the terminal phosphate group was extended in γ-ester derivatives of UTP. The potent N^4-benzyloxy derivative **6**, which was 82- and 44-fold $P2Y_6R$-selective *vs.* $P2Y_2$ and $P2Y_4Rs$, respectively,[14] served as the lead compound for a series of 4-oxyimino analogues of cytidine 5′-diphosphate in the present study. Similarly, several *O*-alkyl and aryl ester derivatives[14] of the γ-phosphate of UTP suggested extension in that region as a possible tethering approach for $P2Y_6R$ agonists.

This work has a two-fold goal: (1) the exploration of SAR of pyrimidine nucleotides at the P2YRs leading to a successful strategy for tethering large reporter groups to the pharmacophore, and (2) the characterization of a new fluorescent probe as a useful tool for studying the $P2Y_6R$. We chose to study a fluorescent probe initially using flow cytometry (FCM) and confocal microscopy. Similar to previous studies of fluorescent agonists of the A_{2A} and A_3 adenosine receptors,[18a,34] there was significant internalization of this fluorescent GPCR agonist in $P2Y_6R$-expressing cells.

Results and discussion

Novel nucleotide derivatives for testing at P2YRs (Table 1) were prepared by the synthetic routes shown in Schemes 1 and 2. The nucleotide products for biological testing were purified by HPLC to assure high purity (>95%). The types of nucleotide modifications include: CTP and CDP analogues containing a N^4-alkoxy group (Schemes 1 and 2); Cp_3 analogues containing a substituted γ-alkyl group at the terminal phosphate (Scheme 1). Click chemistry, especially [2 + 3] cycloaddition of acetylene and azide groups,[19] is often used as a linking reaction for preparing conjugates of biologically active small molecules, and therefore, we chose to incorporate alkynyl groups in the nucleotide analogues.

The synthesis of N^4-alkoxycytidines **32**–**38** from cytidine was performed using corresponding alkoxyamines **25**–**31**. The resulting N^4-alkoxycytidines were phosphorylated by standard methods[14,16,20] to give the desired N^4-alkoxycytidine 5′-diphosphates **10**–**15** (Scheme 1). N^4-3-(1,5-Hexadiynyl)-benzyloxycytidine **39** was prepared from N^4-3-iodobenzyloxycytidine **35** using a palladium-catalyzed cross coupling Sonogashira reaction. [21] In each case, the unprotected nucleoside was first treated with phosphorous oxychloride, and after 2 h the reaction mixture was treated with phosphoric acid to produce 5′-diphosphates. The desired N^4-alkoxycytidine 5′-triphosphates **19** and **21** were synthesized from corresponding N^4-alkoxycytidines **32** and **33** after treatment with phosphorous oxychloride followed by bis(tri-*n*-butylammonium) pyrophosphate. The γ-phosphoester derivatives **20**, **22**, and **23** were prepared by the condensation of corresponding alkyl monophosphoric acid with the corresponding N^4-alkoxycytidine 5′-diphosphate in the presence of *N*,*N*′-diisopropylcarbodiimide (DIC).

The fluorescent 5′-diphosphates (N^4-(3-(AlexaFluor-NH-$(CH_2)_6$-triazole-$(CH_2)_2$-C≡C)-benzyloxy))-CDP **16** and N^4-(3-(Cy5-NH-$(CH_2)_6$-triazole-$(CH_2)_2$-C≡C)-benzyloxy)-CDP **17** and model compound γ-(CH_3CONH-$(CH_2)_2$-triazole-$(CH_2)_2$)-N^4-benzyloxy-CTP **24** were synthesized from alkynes **15** and **22** using copper-catalyzed click cycloaddition reactions (Scheme 2).[22] The 5′-monophosphates **42** and **44** corresponding to the two fluorescent analogues **16** and **17**, respectively, were also isolated as byproducts of the reaction.

Functional assays of the nucleotide analogues (Table 1) consisted of measuring potency for activation of phospholipase C (PLC) in 1321N1 human astrocytoma cells stably expressing the human (h) $P2Y_6R$ (1321N1-$P2Y_6R$ cells),[23] and selectivity was assessed by quantification of PLC activation in 1321N1 cells stably expressing the $hP2Y_2R$ or $hP2Y_4R$. Previously reported data for 5′-diphosphate analogue **6**, dinucleotides **7** and **8**, and 5′-triphosphate analogues **19** and **21** were included for comparison (Table 1).[14]

High potency at the $P2Y_6R$ was achieved with N^4-benzyloxycytidine 5′-diphosphates, including various benzyl-substituted analogues. Halogenated analogues **10**–**13** were compared with **14**, which has a strong electron withdrawing nitro group and is highly selective for the $P2Y_6R$. 3-Bromo derivative **10** was 160- and >260-fold selective toward the $P2Y_6R$, in comparison to the $P2Y_2R$ and $P2Y_4R$, respectively. N^4-(3-iodobenzyloxy)-CDP (**11**, EC_{50} 19 nM) was more potent than the corresponding 4-iodo isomer **13**. This finding led to the introduction at the N^4 position in **15** of a terminal alkyne for tethering a sterically bulky group by click chemistry. $P2Y_6R$ potency was largely retained in this 3-dialkyne, with an EC_{50} value of 100 nM and at least one order of magnitude subtype selectivity. In general, the 5′-diphosphate derivatives containing various N^4-benzyloxy substitutions at the *m*- or *p*-position were potent and selective at the $P2Y_6R$, suggesting that this region of the ligand protrudes outside of the steric and electronic constraints of the principal binding site. The $P2Y_6R$ selectivity of fluorescent agonist **16** in comparison to the $P2Y_2R$ and $P2Y_4R$ was 280- and >1100-fold, respectively. This was especially striking, and its potency surpassed that of the immediate precursor **15** lacking the fluorophore by 11-fold. However, among

dinucleoside triphosphate derivatives, the enlargement of the N^4-methyloxy in **8** to N^4-benzyloxy in **18** reduced both potency and selectivity at the $P2Y_6R$.

UDP and its 5′-diphosphate derivatives are known to potently activate the $P2Y_{14}R$.[40] However, CDP analogues containing a N^4-alkoxy group were shown to be only weakly active at this subtype.[14] Consistently, **16** at concentrations up to 10 μM did not activate the $hP2Y_{14}R$ to inhibit forskolin-stimulated adenylate cyclase (in C6 rat glioma cells stably expressing the receptor,[40] Fig. S1[†]). Thus, the Alexa Fluor 488 conjugate **16** promises to be a potent and relatively selective ligand probe of the $P2Y_6R$.

Derivatization at the γ-phosphate moiety of 5′-triphosphates was less favorable than at the N^4 position for retention of potency and selectivity at the $P2Y_6R$. A naphthyl ester of the γ-phosphate moiety **20** failed to enhance potency at the $P2Y_6R$ in comparison to **19**. Several alkynyl γ-phosphoester model compounds exhibited substantially reduced $P2Y_6R$ potency in comparison to the corresponding 5′-triphosphate **21**. A terminal alkynyl ester **22** was significantly more potent than the higher homologue **23**, which was nearly inactive at the $P2Y_6R$. A model click product, triazole **24** with an amide-containing terminal chain, had improved potency compared to precursor **23** but still had an EC_{50} value of only 879 nM.

Thus, the pyrimidine N^4 position of CDP was thought to provide a better prospect than the γ-phosphate moiety of CTP derivatives, for chain extension with retention of potency at the $P2Y_6R$. N^4-linked fluorescent conjugates, such as the Alexa Fluor 488 conjugate **16**, were considered for use as fluorescent probes in assays using 1321N1-$P2Y_6R$ cells. Compound **16** proved to be a useful fluorescent probe for FCM, a technique that has proven effective for studying other GPCRs in intact cells.[18] The fluorescent dye Alexa Fluor 488 is a suitable fluorophore for FCM binding assays and live cell imaging.[18,34]

The visible fluorescence spectrum of aqueous **16** displayed absorption and emission maxima at 494 and 518 nm, respectively (ESI, Fig. S2[†]). This fluorescent probe was initially tested in FCM after a long incubation period to allow internalization. A FCM histogram of the total binding and nonspecific binding to 1321N1-$P2Y_6R$ cells using 400 nM **16** after 3 h incubation is shown in Fig. 1A. The peak for total binding was significantly higher than the autofluorescence and was located within the optimal window for analysis, but it was not completely separated from the peak for auto-fluorescence. However, the corresponding fluorescent 5′-monophosphate **42** at the same concentrations did not label the cells during a 60 min incubation (Fig. 1B–E and S3[†]). This is consistent with the inactivity of 5′-monophosphate derivatives in general at the $P2Y_6R$. There was no specific labeling by **16** or **42** of control 1321N1 cells. Also, we observed no specific labeling by **16** of 1321N1 cells expressing the $hP2Y_1R$ (data not shown).

Increasing the concentration of **16** from 10 nM to 10 μM increased fluorescent labeling of 1321N1-$P2Y_6R$ cells during a 60 min incubation, and a comparison by FCM of specific and nonspecific binding shows a clear separation over a wide concentration range (10 nM to 1.5 μM, 3 h incubation at 37 °C, Fig. 2A). The fluorescence values were converted to molecules

[†]Electronic supplementary information (ESI) available. See DOI: 10.1039/c3md00132f

of equivalent soluble fluorochrome (MESF).[18] Cells expressing the $P2Y_6R$ in the absence of **16** were used to measure cellular autofluorescence. Nonspecific binding of **16** was measured in the presence of 100 μM UDP, and the ratio of specific to nonspecific binding was high (~4 : 1 at 500 nM **16**). Fluorescent labeling of the cells with **16** approached saturation. The measured cell fluorescence is a composite of the surface-bound and the internalized fluorescence due to the agonist nature of **16**. Therefore, it was not possible to calculate an apparent equilibrium binding constant (K_d) from this curve, which represents a multistep process. Also, the metabolic stability of these nucleotide derivatives was not studied; it is possible that hydrolysis of the diphosphate during the incubations affects the fluorescent labeling of whole cells.

Another fluorophore (Cy5) with a longer emission wave-length than Alexa Fluor 488 was introduced in **17** at the same position as Alexa Fluor 488 in **16**. Unfortunately, the labeling of 1321N1 astrocytoma cells with **17** (100 nM to 1 μM) was independent of the expression of the $P2Y_6R$, and it could not be blocked by 100 μMUDP (Fig. S4†). Therefore, this conjugate was not suitable for further studies of $P2Y_6R$ labeling.

Kinetics of cell labeling by **16** was also determined using a FCM assay (Fig. 2B). Binding of 400 nM **16** to 1321N1-$P2Y_6R$ cells approached a maximum slowly, as observed previously with a fluorescent antagonist of the hA_3 adenosine receptor.[18] An association rate constant (k_1) was determined to be 0.019 min^{-1} (Fig. S5†). Nonspecific $P2Y_6R$ binding was measured in the presence of 100 μM UDP, the surface bound fraction was measured with incubation of 0.4 M sucrose-containing media, and the internalized ligand was measured as the acid-insensitive fraction following acid wash. The internalization of the $P2Y_6R$ (determined by the comparison of the acid-insensitive fraction and the total binding) occurred with a $t_{1/2}$ of 18 min. The fraction of fluorescence associated with the internalized label was much greater (77% of the total binding) than the fraction on the cell surface (17% of the total binding) at the end of the 60 min incubation period (Fig. 2C).

In confocal microscopy, after 60 min incubation at 37 °C, the cell-associated fluorescence of compound **16** (2 μM) in 1321N1-$P2Y_6R$ cells was receptor-dependent and mainly intracellular, providing further evidence of $P2Y_6R$ internalization upon agonist binding (Fig. 3). Also, the addition of hyperosmolaric sucrose to the medium clearly left the fluorescent labeling on the cell surface and prevented its internalization. The appearance of the labeling on the cell surface in Fig. 3C is punctate, suggesting that the receptor is organized into concentrated regions on the cell surface rather than being evenly distributed. Micrographs in Fig. 4 illustrate the ability of known $P2Y_6R$ ligands, agonist **8** and diisothiocyanate antagonist MRS2578, to inhibit fluorescent labeling in 1321N1-$P2Y_6R$ cells by compound **16**. Several known $P2Y_6R$ ligands were compared for the ability to inhibit the fluorescent binding of **16** to 1321N1-$P2Y_6R$ cells were compared after a 30 min pre-incubation followed by a brief treatment with the fluorescent ligand **16** (2 min). Agonists UDP (10 μM) and MRS2957 (0.5 μM) and antagonist MRS2578 (1 μM) caused a significant reduction of labeling determined using FCM (Fig. S6†).

Other fluorescent agonist ligands for GPCRs have been characterized, such as adenosine receptor agonists,[24,34] which internalized in a similar fashion.[34] It has been shown that a

fluorescently labeled A_{2A} adenosine receptor agonist Alexa488-APEC internalized upon agonist stimulation *via* clathrin-coated pit endocytosis, promoting a localization of the receptor in Rab5-positive early endosomes in both CHO and HEK293 cells.[34] It was also demonstrated that desensitization of the $P2Y_6R$ is delayed compared to the $P2Y_4R$,[35] and that prolonged incubation with UDP caused a loss of surface $P2Y_6R$, and rapid recovery of surface $P2Y_6R$ did not occur following removal of the agonist.[36] The desensitization and internalization of two other Gq-coupled receptors, $P2Y_2R$ and $P2Y_4R$, have also been described.[36–38] Nevertheless, in this study the fluorescent agonist **16** was clearly internalized in $P2Y_6R$-expressing cells.

Molecular modeling was used to probe the structural basis for the significantly enhanced potency and selectivity of the Alexa Fluor conjugate **16**. To generate a hypothesis of the interactions of the fluorescent ligand **16** with the receptor, we constructed a new $P2Y_6R$ model based on our recently published homology model of the $P2Y_4R$, constructed using the CXCR4 chemokine receptor structure as a template.[20,25] As we explained recently,[20,26] among the GPCRs structures that have been solved crystallographically, the CXCR4 receptor appears to be a suitable template for the modeling of the P2YRs, since it is relatively close in sequence and shares common structural features with P2YRs. It was first necessary to align the sequences of the two receptors (Fig. S7[†]). After the construction of the model, we subjected the fluorescent ligand **16** to a Monte Carlo Multiple Minima (MCMM) conformational search within the binding cavity of the $P2Y_6R$, granting full flexibility to this ligand as well as all of the surrounding amino acid residues. The conformational search suggested that while the nucleotide portion of the fluorescent ligand bound rigidly to the receptor, the large N^4 substituent retains some flexibility (Fig. 5A). Specifically, it suggested that the nucleotide portion of the fluorescent ligand bound to the receptor with a mode consistent with that seen in our previous models of the P2YRs (Fig. 5B).[12,20,27–29] In particular, the 5′-diphosphate moiety of the ligand interacts, in our model, with three cationic residues located in TM3, TM6 and TM7: Arg103$^{3.29}$, Lys259$^{6.55}$ and Arg287$^{7.39}$ (using a standard numbering convention[30]). These residues are conserved as cationic residues in all subtypes of the $P2Y_1$-like subfamily of the P2YRs and, according to mutagenesis data gathered for the $P2Y_1$ and $P2Y_2$Rs, are fundamental for ligand recognition.[31–33] A fourth cationic residue located in TM7 and conserved as a Lys in all the subtypes of the $P2Y_1$-like receptors that bind uracil nucleotides, namely Lys284$^{7.36}$ in the $P2Y_6R$, interacted in the model with the phosphate as well as with the pyrimidine base of the ligand.

The conformational search also suggested that the large N^4 substituent of **16** protruded from the interhelical binding cavity of the receptor toward the extracellular space to wrap around the second extracellular loop and to end in proximity of the extracellular portion of TM3, interacting with Asp96$^{3.22}$ and Arg100$^{3.26}$ (Fig. 5C). Notably, a visualization of the molecular surface of the residues that surround the extended N^4 substituent, colored according to their electrostatic potential, suggested a substantial steric and electrostatic complementarity between the distal portions of the ligand and the receptor. A sulfonate group of the Alexa Fluor 488 forms an electrostatic interaction with R100, and an amino group is in proximity to Asp96 (both in TM3 near EL2). By analogy, the enhanced affinity

of a fluorescent probe for the A_3 adenosine receptor also correlated with predicted charged interactions of a bulky Alexa Fluor 488 moiety with EL2.[18]

Conclusions

In an effort to functionalize a $P2Y_6R$ agonist for fluorescent labeling, we probed two positions of pyrimidine nucleotides by introducing various functional groups, including alkynes for click chemistry. Functionalization of extended imino substituents at the N^4 position of the pyrimidine nucleobase of CDP retained $P2Y_6R$ potency to a higher degree than γ-phosphoester formation in UTP derivatives. Thus, we have identified a pyrimidine N^4-alkoxy group as a site for tethering $P2Y_6R$ agonists to a fluorescent label. The bifunctional conjugate **16** containing a fluorophore (Alexa Fluor 488) and spacer chain constructed through click chemistry, was potent and selective agonist at the $P2Y_6R$. It was suitable for the study of binding and internalization kinetics on whole cells using FCM and microscopy. The binding of **16** to purified membranes of cells overexpressed the $P2Y_6R$ remains to be characterized. Thus, we introduce the first high affinity fluorescent ligand specific for a P2YR, although additional pharmacological characterization to define the complex cell labeling is needed.

Based on the bulk tolerance of some of these nucleotide derivatives, the functionalized chain appears to be accessing the extracellular regions of the receptor. Although only one fluorescent conjugate **16** showed high potency at the $P2Y_6R$, this site on the nucleotide promises to be a general site for derivatization with bulky substituents, including other fluorophores and specialized reporter groups for receptor detection and characterization.[39] A molecular modeling study was carried out to explore the recognition of the agonist **16** in binding to the $P2Y_6R$ to highlight the key putative interactions between charged groups of a large fluorophore moiety and the outer regions of TM3 in the $P2Y_6R$, which evidently enhance the potency of **16**. In conclusion, we have identified the N^4-benzyloxy group as a structurally permissive region for synthesis of a family of functionalized congeners as fluorescent conjugates and other pharmacological probes for studying the $P2Y_6R$. This will enable further drug discovery related to this receptor.

Supplementary Material

Refer to Web version on PubMed Central for supplementary material.

Acknowledgments

This research was supported in part by the Intramural Research Program of the NIH, National Institute of Diabetes and Digestive and Kidney Diseases and a grant (GM38213) from the National Institute of General Medical Sciences. We thank Noel Whittaker (NIDDK) for mass spectral determinations. EK thanks the Hungarian-American Enterprise Scholarship Foundation (HAESF) for financial support. LS thanks the University of Florence, Italy for financial support.

Abbreviations

1321N1-P2Y6R cells	1321N1 Human astrocytoma cells expressing the human $P2Y_6$ receptor

CDP	Cytidine, 5′-diphosphate
CTP	Cytidine 5′-triphosphate
DCC	*N*,*N*′-Dicyclohexylcarbodiimide
DIC	*N*,*N*′-Diisopropylcarbodiimide
DMF	*N*,*N*-Dimethylformamide
EDC	*N*-(3-Dimethylaminopropyl)-*N*′-ethylcarbodiimide
FCM	Flow cytometry
GPCR	G protein-coupled receptor
HBSS	Hank's balanced salt solution
HEPES	*N*-2-Hydroxyethylpiperazine-*N*′-2-ethanesulfonic acid
HPLC	High performance liquid chromatography
MCMM	Monte Carlo Multiple Minima
MESF	Molecules of equivalent soluble fluorochrome
MRS2957	P^1-(Uridine 5′-)-P^4-(N^4-methoxycytidine 5′-) triphosphate
MRS2578	*N*,*N*′-1,4-butanediyl*bis*[*N*′-(3-isothiocyanatophenyl)thiourea
P2YR	P2Y receptor
PLC	Phospholipase C
SAR	Structure activity relationship
TBAP	Tetrabutylammonium dihydrogenphosphate
TEAA	Triethylammonium acetate
THF	Tetrahydrofuran
TLC	Thin layer chromatography
TM	Transmembrane helical domain
UDP	Uridine 5′-diphosphate
UTP	Uridine 5′-triphosphate

Notes and references

1. Abbracchio MP, Burnstock G, Boeynaems JM, Barnard EA, Boyer JL, Kennedy C, Knight GE, Fumagalli M, Gachet C, Jacobson KA, Weisman GA. Pharmacol Rev. 2006; 58:281–341. [PubMed: 16968944]
2. Vieira RP, Müller T, Grimm M, von Gernler V, Vetter B, Dürk T, Cicko S, Ayata CK, Sorichter S, Robaye B, Zeiser R, Ferrari D, Kirschbaum A, Zissel G, Virchow JC, Boeynaems JM, Idzko M. Am J Respir Crit Care Med. 2011; 184:215. [PubMed: 21512170]
3. Mamedova LK, Wang R, Besada P, Liang BT, Jacobson KA. Pharmacol Res. 2008; 58:232. [PubMed: 18805489]

4. Balasubramanian R, Ruiz de Azua I, Wess J, Jacobson KA. Biochem Pharmacol. 2010; 79:1317. [PubMed: 20067775]
5. Orriss IR, Wang N, Burnstock G, Arnett TR, Gartland A, Robaye B, Boeynaems JM. Endocrinology. 2011; 152:3706. [PubMed: 21828185]
6. Koizumi S, Shigemoto-Mogam Y, Nasu-Tada K, Shinozaki Y, Ohsawa K, Tsuda M, Joshi BV, Jacobson KA, Kohsaka S, Inoue K. Nature. 2007; 446:1091. [PubMed: 17410128]
7. Grbic DM, Degagné E, Larrive JF, Bilodeau MS, Vinette V, Arguin G, Stankova V, Gendron FP. Inflammatory Bowel Dis. 2012; 18:1456.
8. Markovskaya A, Crooke A, Guzmán-Aranguez AI, Peral A, Ziganshin AU, Pintor J. Eur J Pharmacol. 2008; 579:93. [PubMed: 18031728]
9. Bar I, Guns PJ, Metallo J, Wilkin F, Cammarata D, Boeynaems JM, Bult H, Robaye B. Mol Pharmacol. 2008; 74:777. [PubMed: 18523137]
10. Uratsuji H, Tada Y, Kawashima T, Kamata M, Hau CS, Asano Y, Sugaya M, Kadono T, Asahina A, Sato S, Tamaki K. J Immunol. 2012; 188:436. [PubMed: 22102722]
11. El-Tayeb A, Qi A, Müller CE. J Med Chem. 2006; 49:7076. [PubMed: 17125260]
12. Besada P, Shin DH, Costanzi S, Ko HJ, Mathé C, Gagneron J, Gosselin G, Maddileti S, Harden TK, Jacobson KA. J Med Chem. 2006; 49:5532–5543. [PubMed: 16942026]
13. Ginsburg-Shmuel T, Haas M, Schumann M, Reiser G, Kalid O, Stern N, Fischer B. J Med Chem. 2010; 53:1673. [PubMed: 20095577]
14. Maruoka H, Barrett MO, Ko H, Tosh DK, Melman A, Burianek LE, Balasubramanian R, Berk B, Costanzi S, Harden TK, Jacobson KA. J Med Chem. 2010; 53:4488. [PubMed: 20446735]
15. Shaver SR, Rideout JL, Pendergast W, Douglass JG, Brown EG, Boyer JL, Patal RI, Redick CC, Jones AC, Picher M, Yerxa BR. Purinergic Signalling. 2005; 1:183. [PubMed: 18404503]
16. Ko H, Carter RL, Cosyn L, Petrelli R, de Castro S, Besada P, Zhou Y, Cappellacci L, Franchetti P, Grifantini M, Van Calenbergh S, Harden TK, Jacobson KA. Bioorg Med Chem. 2008; 16:6319. [PubMed: 18514530]
17. El-Tayeb A, Qi A, Nicholas RA, Müller CE. J Med Chem. 2011; 54:2878. [PubMed: 21417463]
18. (a) Kozma E, Kumar TS, Federico S, Phan K, Balasubramanian R, Gao ZG, Paoletta S, Moro S, Spalluto G, Jacobson KA. Biochem Pharmacol. 2012; 83:1552. [PubMed: 22402302] (b) Kozma E, Gizewski ET, Tosh DK, Squarcialupi L, Auchampach JA, Jacobson KA. Biochem Pharmacol. 2013; 85:1171. [PubMed: 23376019]
19. Moses JE, Moorhouse AD. Chem Soc Rev. 2007; 36:1249. [PubMed: 17619685]
20. Maruoka H, Jayasekara MPS, Barrett MO, Franklin DA, de Castro S, Kim N, Costanzi S, Harden TK, Jacobson KA. J Med Chem. 2011; 54:4018. [PubMed: 21528910]
21. Chinchilla R, Nájera C. Chem Rev. 2007; 107:874. [PubMed: 17305399]
22. Tosh DK, Yoo LS, Chinn M, Hong K, Kilbey SM, Barrett MO, Fricks IP, Harden TK, Gao ZG, Jacobson KA. Bioconjugate Chem. 2010; 21:372.
23. Bourdon DM, Wing MR, Edwards EB, Sondek J, Harden TK. Methods Enzymol. 2006; 406:489. [PubMed: 16472681]
24. Dale CL, Hill SJ, Kellam B. Med Chem Commun. 2012; 3:333.
25. Wu B, Chien EY, Mol CD, Fenalti G, Liu W, Katritch V, Abagyan R, Brooun A, Wells P, Bi FC, Hamel DJ, Kuhn P, Handel TM, Cherezov V, Stevens RC. Science. 2010; 330:1066. [PubMed: 20929726]
26. Deflorian F, Jacobson KA. J Comput-Aided Mol Des. 2011; 25:329. [PubMed: 21461952]
27. Costanzi S, Mamedova L, Gao ZG, Jacobson KA. J Med Chem. 2004; 47:5393. [PubMed: 15481977]
28. Costanzi S, Joshi B, Maddileti S, Mamedova L, Gonzalez-Moa M, Marquez V, Harden TK, Jacobson KA. J Med Chem. 2005; 48:8108. [PubMed: 16366591]
29. Jacobson KA, Costanzi S, Ivanov A, Tchilibon S, Besada P, Gao Z, Maddileti S, Harden TK. Biochem Pharmacol. 2006; 71:540. [PubMed: 16359641]
30. Ballesteros JA, Weinstein H. Methods Neurosci. 1995; 25:366.

31. Hillmann P, Ko GY, Spinrath A, Raulf A, von Kügelgen I, Wolff SC, Nicholas RA, Kostenis E, Höltje HD, Müller CE. J Med Chem. 2009; 52:2762. [PubMed: 19419204]
32. Moro S, Guo D, Camaioni E, Boyer JL, Harden TK, Jacobson KA. J Med Chem. 1998; 41:1456. [PubMed: 9554879]
33. Jiang Q, Guo D, Lee BX, Van Rhee AM, Kim YC, Nicholas RA, Schachter JB, Harden TK, Jacobson KA. Mol Pharmacol. 1997; 52:499. [PubMed: 9281613]
34. Brand F, Klutz A, Jacobson KA, Fredholm BB, Schulte G. Eur J Pharmacol. 2008; 590:36. [PubMed: 18603240]
35. Robaye B, Boeynaems JM, Communi D. Eur J Pharmacol. 1997; 329:231. [PubMed: 9226417]
36. Brinson AE, Harden TK. J Biol Chem. 2001; 276:11939. [PubMed: 11114308]
37. Flores RV, Hernández-Pérez MG, Aquino E, Garrad RC, Weisman GA, Gonzalez FA. Mol Cell Biochem. 2005; 280:35. [PubMed: 16311903]
38. Sromek SM, Harden TK. Mol Pharmacol. 1998; 54:485. [PubMed: 9730907]
39. Jacobson KA. Bioconjugate Chem. 2009; 20:1816.
40. Carter RL, Fricks IP, Barrett MO, Burianek LE, Zhou Y, Ko H, Das A, Jacobson KA, Lazarowski ER, Harden TK. Mol Pharmacol. 2009; 76:1341. [PubMed: 19759354]

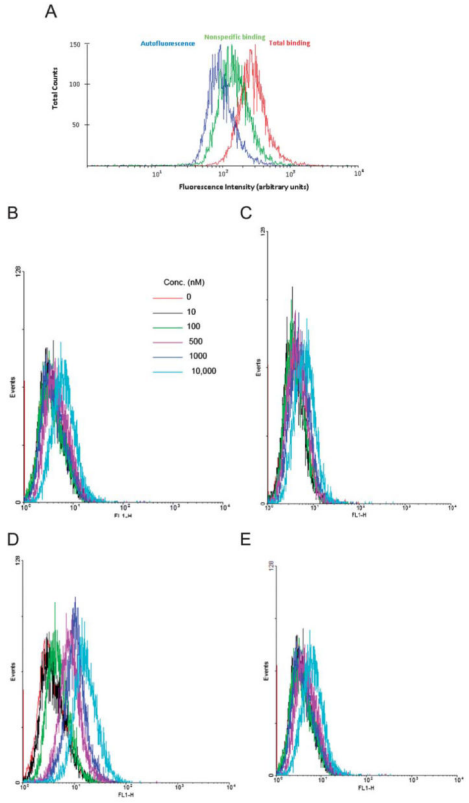

Fig. 1.

(A) FCM histogram following 3 h incubation of 1321N1 astrocytoma cells expressing the $P2Y_6R$ in 400 nM **16** (MRS4129), showing the total binding (red), autofluorescence (blue) and nonspecific binding (green). The histogram represents data of one of the three independent experiments. (B–E) FCM histograms following 60 min incubation of: (B) control 1321N1 astrocytoma cells with various concentrations of $P2Y_6R$ agonist **16**; (C) control 1321N1 astrocytoma cells with various concentrations of inactive 5′-monophosphate derivative **42**; (D) 1321N1 astrocytoma cells expressing the $P2Y_6R$ with various concentrations of $P2Y_6R$ agonist **16**; (E) 1321N1 astrocytoma cells expressing the $P2Y_6R$ with various concentrations of inactive 5′-monophosphate derivative **42**.

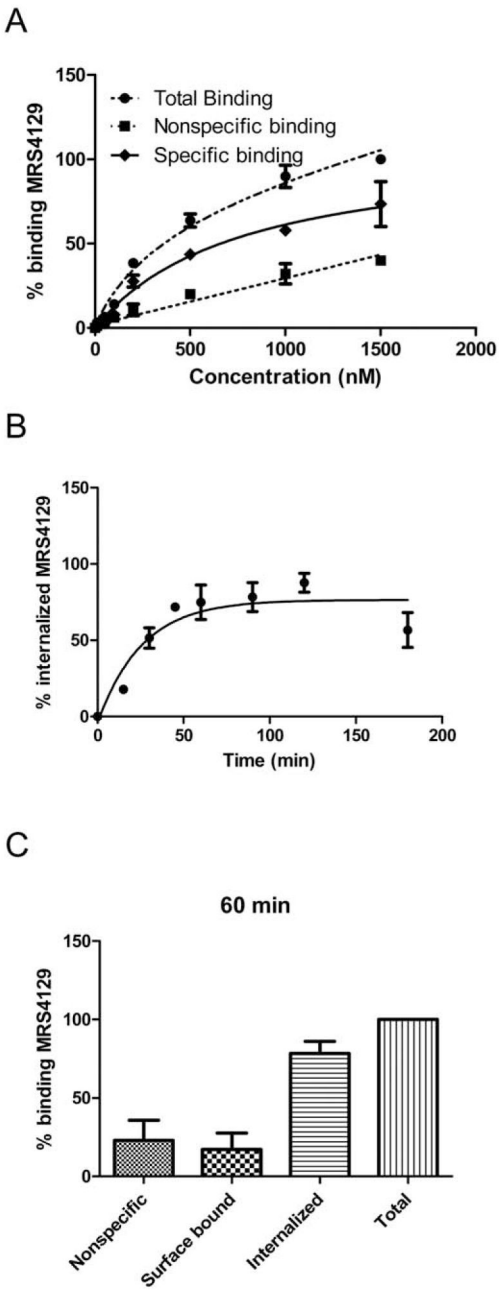

Fig. 2.

(A) Saturation binding experiment with Alexa Fluor 488 conjugate **16** at the $P2Y_6R$ expressed on 1321N1 astrocytoma cells using FCM (3 h incubation). Nonspecific binding was measured in the presence of 100 μM UDP. (B) Internalization kinetics of 400 nM $P2Y_6R$-bound **16** at 37 °C. Internalized amount ($\%_{int}$) was calculated as the acid insensitive fluorescence at *x* time point ($MESF_x$) is compared to total MESF ($MESF_{total}$) corrected with the nonspecific binding ($MESF_{nonspec}$): $\%_{int}=(MESF_x - MESF_{nonspec})/(MESF_{total} - MESF_{nonspec})$. Fluorescence of internalized **16** was measured by FCM after removing cell-surface bound ligand by 3 × 5 min acid wash (pH 3.5). The $t_{1/2}$ of the internalization was 18

min. (C) Comparison of the nonspecifically bound, surface bound, internalized and total bound **16** (sum of surface bound and internalized) after 60 min incubation. In this plot, nonspecific has been subtracted from surface bound, internalized and total bound values. 1321N1-P2Y_6R was incubated with 400 nM fluorescent ligand **16** at 37 °C. Nonspecific binding was measured in the presence of 100 μM UDP, the surface bound fraction was measured with incubation of 0.4 M sucrose-containing media, and the internalized ligand was measured as the acid-insensitive fraction following acid wash. After a 60 min incubation period, the 17% of the total binding was found on the cell surface, 77% was internalized and 23% was nonspecifically bound.

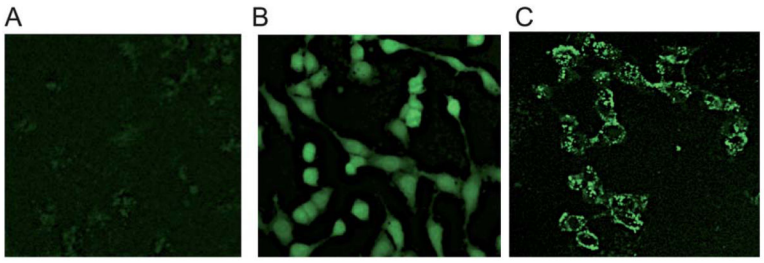

Fig. 3.

Fluorescent micrographs using a Zeiss LSM 700 confocal microscope of $P2Y_6R$-expressing 1321N1 astrocytoma cells exposed to the fluorescent agonist **16** (2 μM, 60 min incubation at 37 °C). (A) Control cells in the absence of **16**; (B) incubation with 1 μM **16** at 37 °C for 60 min in medium without sucrose; (C) incubation with 1 μM **16** at 37 °C for 60 min in medium containing 0.4 M sucrose.

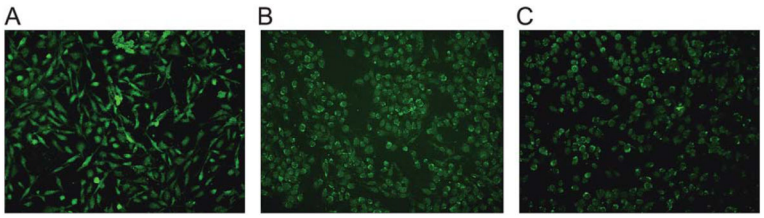

Fig. 4.

Inhibition of fluorescent labeling by known $P2Y_6R$ ligands, using a Keyence BZ-9000 fluorescent microscope equipped with filters for green fluorescence with excitation at 495 nm and emission at 519 nm. Fluorescent micrographs of $P2Y_6R$-expressing 1321N1 astrocytoma cells exposed to (A) the fluorescent agonist **16** (500 nM, 60 min incubation at 37 °C) in the absence of inhibitor or sucrose; (B) same conditions, except a 30 min preincubation with $P2Y_6R$ agonist MRS2957 (**8**, 500 nM) was performed at 37 °C; (C) same conditions, except a 30 min preincubation with $P2Y_6R$ antagonist MRS2578 (500 nM) was performed at 37 °C $P2Y_6R$-expressing 1321N1 astrocytoma cells in the absence of **16** showed a lack of fluorescence, similar to Fig. 3A. Control experiments using 1321N1 astrocytoma cells not expressing a P2YR showed no increase in fluorescence when incubated with **16**.

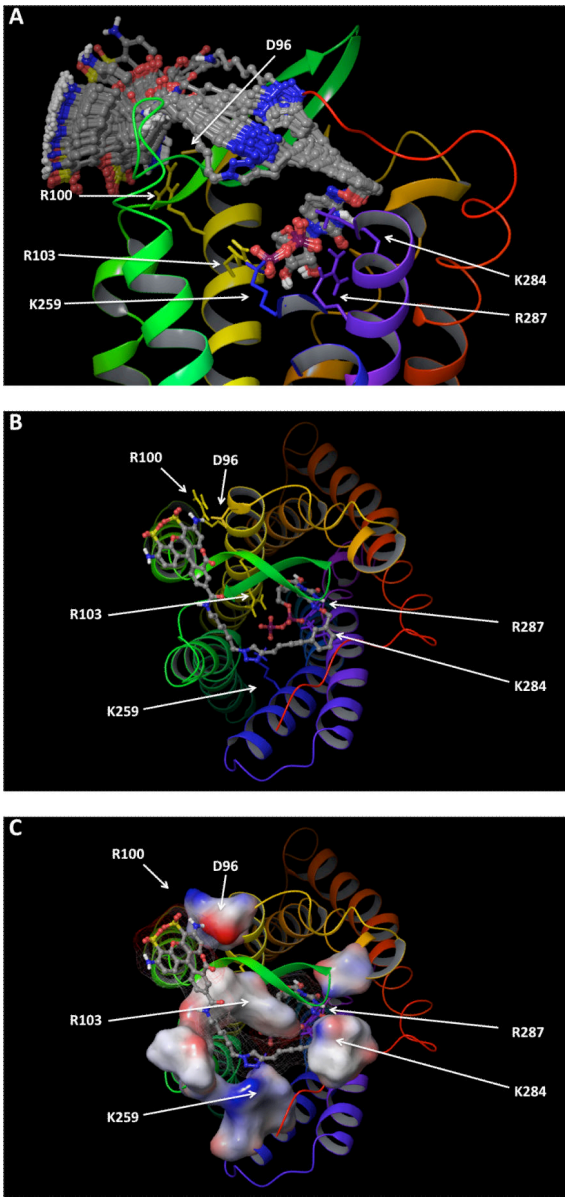

Fig. 5.

Molecular model of the lowest energy conformation of the hP2Y$_6$R complexed with the Alexa Fluor 488-labeled agonist **16**, as obtained after a fully flexible MCMM conformational search, (A) viewed from the plane of the phospholipid bilayer (with other conformations of **16** obtained), or (B) and (C) from the extracellular side. (C) shows the molecular surface of **16** (mesh) and the residues that surround its N^4 substituent (solid), colored by electrostatic potential (red: negative; blue: positive). The schematic representation of the backbone of the receptor is colored by residue number (TM1: orange; TM2: dark yellow; TM3: yellow; TM4 light green; TM5: green; TM6: blue; TM7: purple/blue). The ligand is shown as a ball and stick structure, colored by element (carbon atoms colored in gray). The residues located in proximity to the ligand are labeled and shown as

sticks, colored by residue number. The fluorophore is located near the outer segment of TM3.

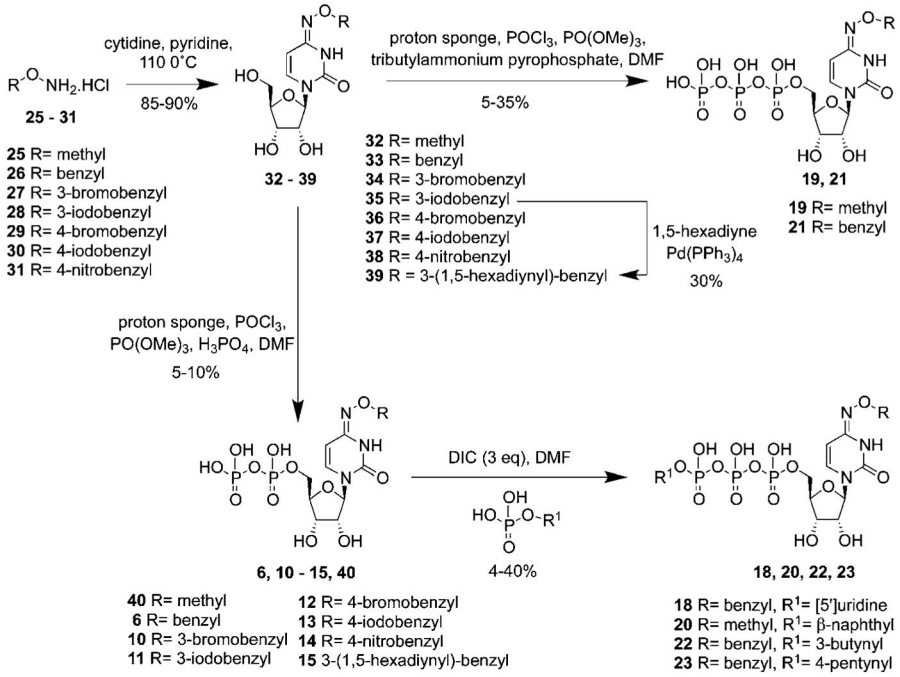

Scheme 1.

Synthesis of various pyrimidine ribonucleoside 5′-tri and 5′-diphosphates.

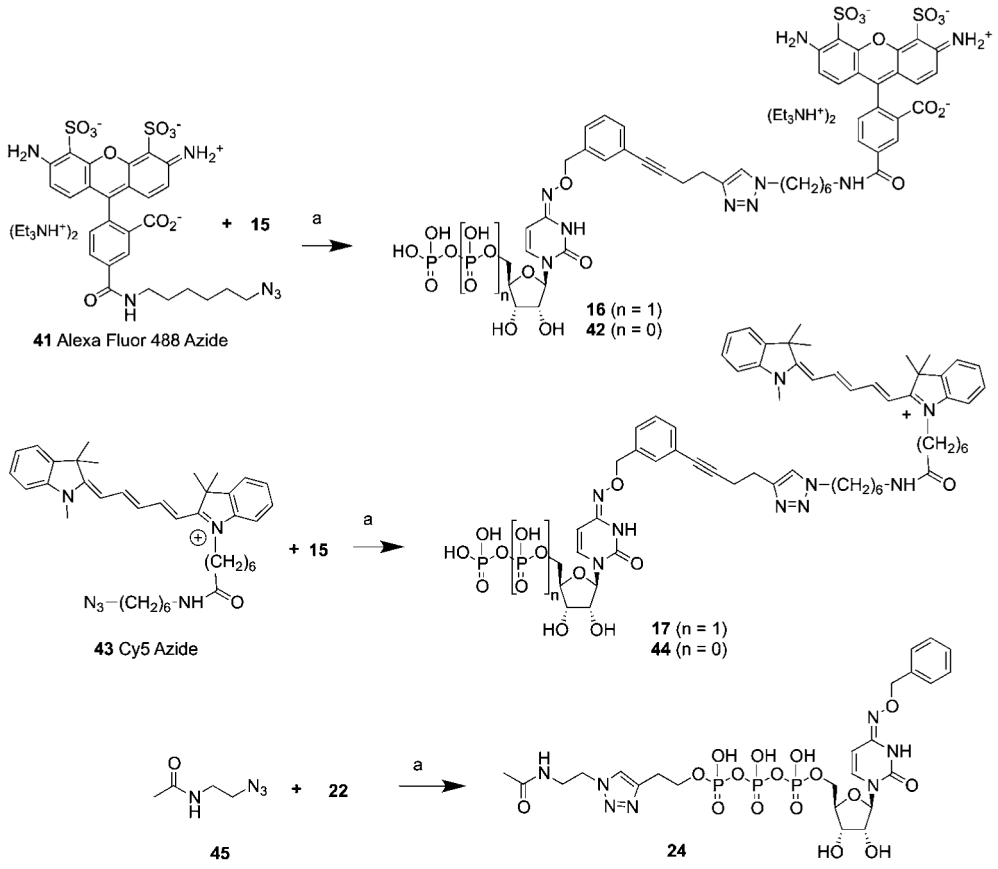

Scheme 2.

Synthesis of fluorescent conjugates **16** and **17** click-linked through the N^4 position and a model compound **24** click-linked through the β-phosphate.

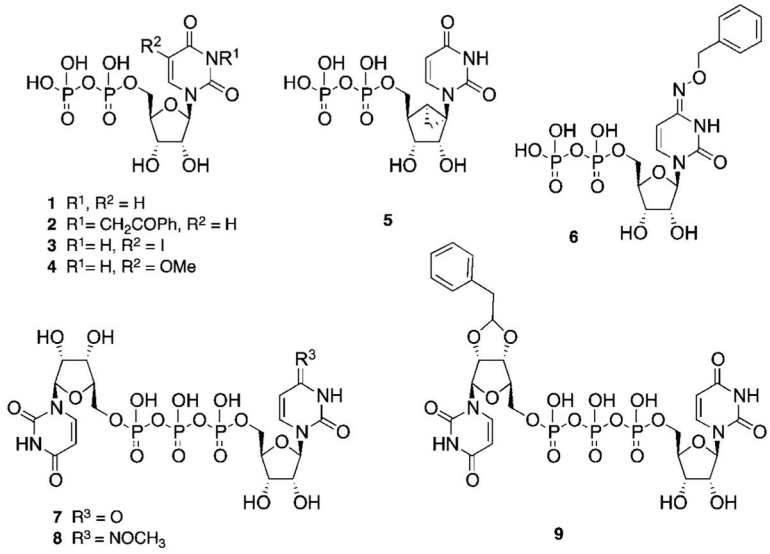

Chart 1.
Structures of prototypical agonist ligands for studying $P2Y_6Rs$.

Table 1

Potency of a series of pyrimidine nucleotide derivatives at three subtypes of hP2YRs

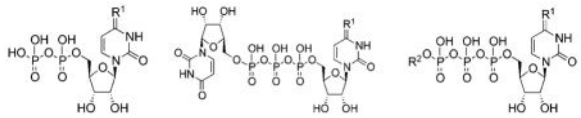

		Potency, EC_{50}, nM or % *activation*		
No.	**Structure, R^1 =**	**P_2Y_6[a]**	**P_2Y_2[a]**	**P_2Y_4[a]**
Diphosphates				
6[b]	=N–O–Bn	26 ± 2	2130 ± 640	1150 ± 150
10	=N–O–(3-Br–Bn)	39 ± 2.2	6200 ± 2100	>10 000
11	=N–O-(3-I–Bn)	19 ± 5	2500 ± 800	352 ± 62
12	=N–O–(4-Br–Bn)	32 ± 4.1	5200 ± 90	7440 ± 500
13	=N–O–(4-I–Bn)	148 ± 37	NE	<50%[c]
14	=N–O–(4-NO_2–Bn)	41 ± 2.0	3300 ± 510	2200 ± 320
15	=N–O–(3-(HC≡C(CH_2)$_2$C≡C)–Bn)	100 ± 11	3900 ± 1200	952 ± 205
16	=N–O–(3-(AlexaFluor–NH–(CH_2)$_6$-triazole–(CH_2)$_2$–C≡C)–Bn)	9 ± 1.9	2500 ± 660	<50%[c]
17	=N–O–(3-(Cy5–NH–(CH_2)$_3$–triazole–(CH_2)$_2$–C≡C)–Bn)	ND	ND	ND
Dinucleoside triphosphates				
7[b,d]	=O	270 ± 70	1310 ± 210	870 ± 110
8[b]	=N–O–Me	12 ± 3	170 ± 40	790 ± 120
18	=N–O–Bn	126 ± 17	1700 ± 500	636 ± 42
Triphosphates and γ-phosphoesters				
Compd	R^1	R^2	P_2Y_6[a]	P_2Y_2[a]	P_2Y_4[a]
19[b]	=N–O–Me	H	130 ± 21	28 ± 4	25 ± 3
20	=N–O–Me	2-Naphthyl	731 ± 28	2900 ± 200	<50%[c]
21[b]	=N–O–Bn	H	230 ± 37	620 ± 75	97 ± 14
22	=N–O–Bn	HC≡C(CH_2)$_2$	1750 ± 280	<50%[c]	<50%[c]

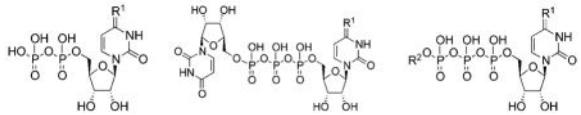

6, 10 – 17 7, 8, 18 19 – 24

			Potency, EC_{50}, nM or % *activation*		
No.	**Structure, R^1 =**		**P_2Y_6[a]**	**P_2Y_2[a]**	**P_2Y_4[a]**
23	=N–O–Bn	$HC{\equiv}C(CH_2)_3$	>10 000	NE	<50%[c]
24	=N–O–Bn	$CH_3CONH–(CH_2)_2$–triazole$(CH_2)_2$	879 ± 32	3800 ± 690	3300 ± 1200

[a] Functional assays were conducted with 1321N1 astrocytoma cells expressing recombinant $hP2Y_2$, $hP2Y_4$, or $hP2Y_6$. Values are expressed as the mean ± SEM. ND, not determined.

[b] Data from Maruoka *et al.*, 2010, 2011.[14,20]

[c] Percent of maximal activation by full agonist at 10 μM.

[d] **7**, Up_3U, **10**, MRS4141; **16**, MRS4129; **17**, MRS4137; **42**, MRS4158 (5′-monophosphate derivative of **16**).

NE – no effect. ND – not determined.